PROCESS SENSITIVITY STUDY OF METAL FUSED FILAMENT FABRICATION (MF^3) USING FINITE ELEMENT-BASED PROCESS SIMULATION APPROACH

Mohammad Qasim Shaikh[1]*, Paramjot Singh[1], Pierre-Yves Lavertu[2], Kunal H Kate[1], Sundar V. Atre[1]

[1]Materials Innovation Guild, University of Louisville, KY 40208, USA.
[2] e-Xstream Engieering, MSC Software Corp (Hexagon), Newport Beach, CA 92660, USA.

Corresponding author: mohammadqasim.shaikh@louisville.edu

ABSTRACT

Metal fused filament fabrication (MF^3) combines fused filament fabrication and sintering processes to fabricate complex metal components. In design for MF^3 ($DfMF^3$), it is important to understand how part design, printing parameters and material properties of filament affect MF^3 printing process in terms of processability, part quality, and ensuing properties. Understanding the interrelationships between material-process-design variations is essential to leverage the potential of MF^3 and deploy it to industrial applications. The goal of the study is to conduct a sensitivity analysis to identify the significance of each input parameter in terms of influence on the output parameters. FEA-based simulations were used to estimate the process outcome in response to variable inputs. However, simulating and optimizing the MF^3 printing process is a complex problem having a number of linked geometry, process and material variables to be considered that influence the process output parameters like deflection, warpage, residual stress, thermal history and print time. Having multiple objective functions for process optimization makes it very difficult to identify critical parameters for designing part geometry, processing conditions and powder-binder feedstock for MF^3. Towards the goal of identifying the level of significance of various input variables during MF^3 process, a systematic procedure for sensitivity analysis has been successfully developed for the printing phase of the MF^3 process. In this sensitivity analysis, all geometry, process and material input variables were varied within a meaningful window one at a time, and influence on process outcome was noted in terms of output parameters. The present sensitivity analysis procedure is expected to be an invaluable tool not only for the materials engineer who has to develop an optimal formulation of MF^3 material, but also for the design engineer who has to determine the critical input parameters for given design targets, as well as for the production engineer who has to optimize and monitor the production stage.

Keywords: metal fused filament fabrication; FEA simulation; process sensitivity; estimations, additive manufacturing design for AM,

Copyright 2020. Used by the Society of the Advancement of Material and Process Engineering with permission.

SAMPE Virtual Conference Proceedings, 2020. Society for the Advancement of Material and Process Engineering – North America.

1. INTRODUCTION

Additive manufacturing (AM) is a technology for fabricating 3D objects by adding material layer upon layer, as opposed to subtractive and formative manufacturing technologies. AM is being increasingly used for fabricating physical objects using polymers, metals, or ceramics, which may be used in various applications [1]. Metal fused filament fabrication (MF^3) is a hybrid AM process used to fabricate custom 3D metal components [2]. The established metal additive manufacturing processes such as laser-powder bed fusion, direct metal laser sintering, and direct energy deposition are energy-intensive and not suited for certain specific requirements like in-space manufacturing. MF^3 provides the best alternative to address these challenges. MF^3 is a multi-step process that involves as shown in Figure 1: (a) mixing and extrusion of a powder-polymer mixture into filaments, (b) 3D printing of a green part, (c) polymer removal from the 3D printed green part by debinding to get a brown part, and (d) densifying the brown part to achieve a fully dense metal part by sintering. MF3 has been found capable of metal additive manufacturing of materials like Ti-6Al-4V, bronze, copper, 17–4 PH stainless steel, 316L stainless steel [3-6].

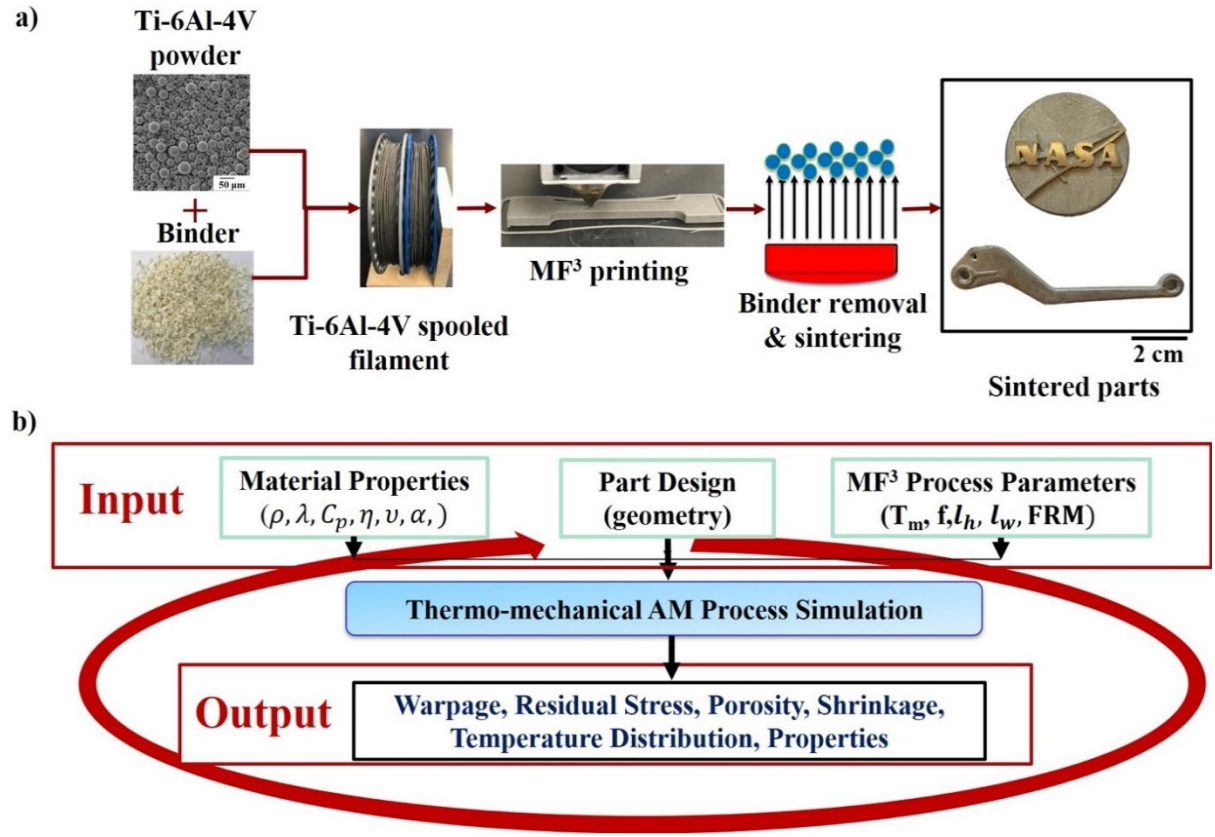


Fig. 1. **a)** Process overview for MF^3 with examples of fabricated Ti-6Al-4V parts by our group and **b) t**he present work for determining the input material parameters for conducting $DfMF^3$.

The material system used in MF^3 comprises an optimum formulation of metal powder mixed with custom polymer binder, like in powder injection molding (PIM). The solids loading and binder composition are varied for different material systems to enable efficient debinding and sintering, or to meet specific application needs [7]. Consequently, the properties of new material may vary considerably. Now, question arise as how these changes in material properties in MF^3 will

influence the process outcome and performance of the end product. The powder-polymer composites are processed by fused filament fabrication (FFF), also known as fused deposition modeling (FDM), which is typically used to get a 3D shape with polymers [1]. This extrusion-based printing process has several variable input parameters like extrusion temperature, build plate temperature, printing speed, layer thickness, extrusion width, toolpath and slicing strategy. These process parameters have significant effects on the printing process as well as printed part quality and performance. The layer-by-layer material deposition develops temperature gradient leading to warpage and residual stresses in printed which are influenced by the process parameters [8,9]. Hence, there is a need for establishing optimized parameters settings for specific materials. The common trial-and-error experimental approach is often costly and time consuming, and sometimes not even feasible. The empirical relationships between input and output parameters are often not straightforward.

Numerical simulation techniques provide effective alternative means to predict the printing process outcome by estimating the thermo-mechanical behavior of 3D parts being printed. [10-14]. The availability of FEA-based simulation tools has shown some promise for aiding the engineer to resolve the inter-related problems involving material-process-geometry in FFF/ FDM process [15,16]. However, the use of such tools to perform material and process simulations of MF^3 is yet to be explored, that will favor the widespread use of the MF^3 process to manufacture parts with different materials for a variety of applications [17].

Understanding the constraints imposed by extrusion based additive manufacturing process and highly filled material used in MF^3 is crucial for successful design and manufacturing. Hence, there is a need for design for MF^3 ($DfMF^3$) approach supported by relevant design tools. Also, development of a product calls for several factors considerations to improve the functional and aesthetic attributes of the part. It may lead to multiple design changes. Here, the questions raise as to how small changes in product and tool dimensions influence process outcome variations. Moreover, any variations in powder-polymer composition can consequently affect filament properties, filament processing, 3D printing, debinding, and sintering. Accordingly, material compositional variations can affect the component geometrical attributes. However, little information is available on the sensitivity of various predictions of CAE simulation tools to variations in the material property values. Additionally, as several process settings need to be changed and controlled during the MF^3 printing process, it is important to understand how a CAE simulation tool captures the influence of such process variations in its predictions.

The above crucial questions are addressed in the current study by analyzing the MF^3 process for the sensitivity of the key output variables to the selected material, geometry and process variables. FEA-based simulations are used to estimate the process outcome in response to variable inputs. CAE simulation tool, Digimat (e-Xstream/ MSC Inc.), was used for integrated thermo-mechanical process simulation [4]. Process simulation helps in predicting and minimizing warpage and residual stresses, achieving intended dimensions through reverse warpage, and estimating the structural performance of the 3D printed parts. The quantitative relationships on the dependence of many MF^3 process output parameters on changes in component geometry, process parameters and material properties are presented. The dimensionless sensitivity factor allows the parameters with different units to be compared quantitatively with a single yardstick. It also facilitated the identification of dominant input parameters and relative contribution to each output parameter. The results provide important insights into the geometry-process-material interrelationships in the MF^3 process.

The study provides a powerful approach that can be applied to identify the parameters that need to be optimized in the design stage and carefully monitored and controlled in the production stage. We anticipate that the sensitivity analysis tool presented in this paper will be a valuable tool for the design and production engineer in the additive manufacturing industry. Also, during material formulation development the tool can provide insights about sensitivity evolution with different solids loading and binder compositions to optimize the formulations. The simulations in this study only focused on the printing stage of the MF^3 process, as simulation solutions for debinding and sintering process are under development.

1.1 FEA simulation of MF^3 process

In this study, the commercially available software, Digimat was used to carry out the finite element-based (FE) process simulations of MF^3 printing process. The tool provides the capability of using indirect sequentially coupled thermomechanical analysis for both stress and heat analysis [26]. It enables numerical analyses of the complex thermomechanical loadings that occur during the layer-by-layer deposition of the material, successive cooling of the part and thermal history of the material deposition that generates differential shrinkage between adjacent beads or layers that shapes the part. Through the element activation/deactivation function in the Digimat, a small part of the geometry was activated sequentially that represents filament-wise printing that progresses layer-by-layer [29]. Once all the elements were activated, the final results are then used for a thermomechanical coupled analysis in order to simulate the solidification process and the cooling phase. Extrusion based printing of higher filled powder polymer mixture in MF^3 exhibits strong dependency of the filament material thermal, mechanical and physical properties. In this study, the properties used for Ti-6Al-4V in custom polymer binder were obtained from estimation models [2]. The FE simulations were used to estimate the process time, deflection/ warpage, residual stresses and thermal history that take place in the printing process. These estimations can enable design and process engineers to not only come-up with optimal material, design and processing parameters but also identify potential issues and troubleshoot them at the early stage of design.

2. METHODOLOGY

The simulations in this study only focused on the printing stage of the MF^3 process. Simulation solutions for debinding and sintering stages of the MF^3 process are being developed and will be reported separately. Five different component geometries were selected and simulated: thin walled components (Figure 2A-D), and solid component (Figure 2E). Starting with a thin-walled hollow structure, designs were evolved to evaluate sensitivity with changing part size, volume, thickness, height, layer surface area, and structural stiffness. In the present study, only Design-I was studied in detail, while other four designs and evolution sensitivity with changing geometries will be presented in future.

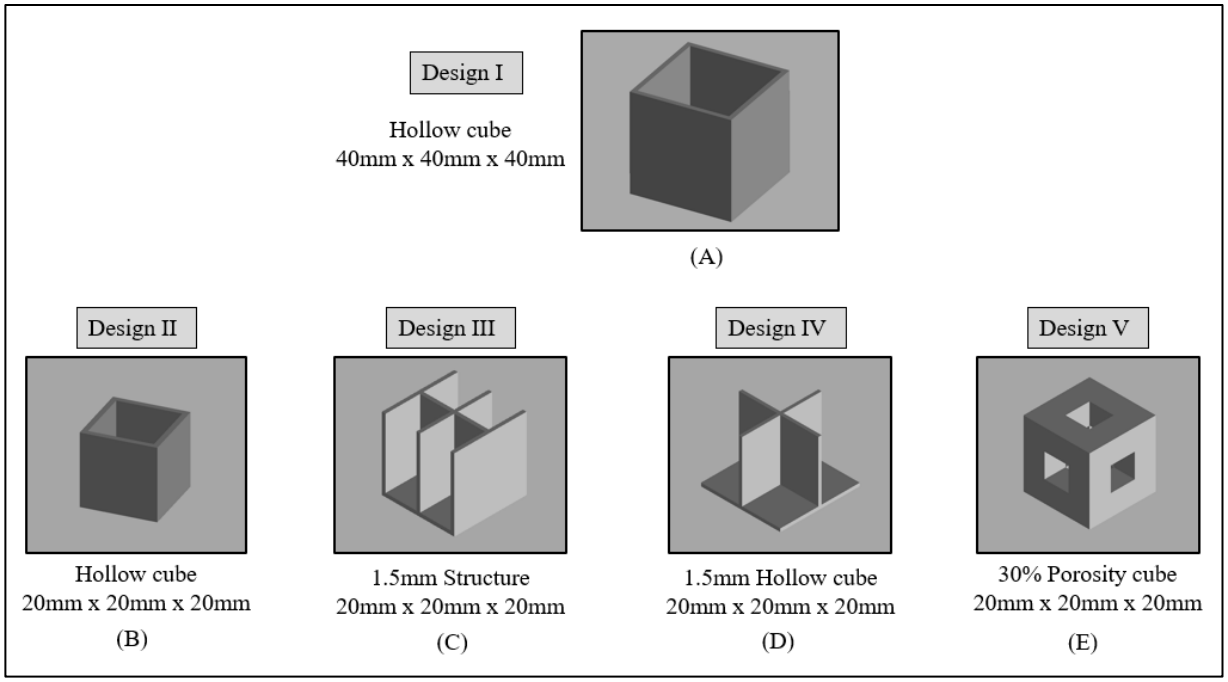


Figure 2. Five different part designs used for simulation in the study.
(A-D) Thin walled components (E) Solid component

An optimal formulation of Ti-6Al-4V in custom polymer binder was developed by our research group for MF^3 [2]. The same material was evaluated in this sensitivity study. The material definition for simulation includes mechanical and thermal properties over a range of temperature. A CAD model in STL format defines the part geometry. It was discretized into voxel mesh. Voxel mesh size is decided according to layer thickness and part geometry. A GCode file from a slicing tool, Simplify3D, defines toolpath, layer thickness and printing speed. Other printing parameters like layer width, extrusion temperature, build plate temperature, chamber temperature, convection coefficient are defined through simulation tool graphical user interface. Having material, geometry and process input defined, thermo-mechanical simulations were performed for each of the five geometries.

For each of the designs, first a base case MF^3 printing process was studied with given geometry, typical values of material properties, and process parameters as input parameters. Then, each of the geometry, process and material input variables was varied within a meaningful window one at a time, and the influence on process outcome was noted. For each input variation a simulation job was performed, and simulation results are reported as output parameters.

The input parameters for this study have been divided into three subgroups:

- component geometry parameters
- process parameters
- material properties

The output parameters evaluated in the study include:

- print time
- deflection
- Z-warpage
- residual stresses
- temperature distribution

The goal of this sensitivity analysis is to evaluate the sensitivity of output parameters to each of input parameters, and subsequently identify input parameters that have the greatest influence on each of the output parameters in MF^3 printing process.

Sensitivity analysis

For the sensitivity analysis, each of the input parameters was varied over a range of interest and feasibility. The response of each output parameter was recorded to evaluate its sensitivity to variation in input parameters. The sensitivity was calculated as the gradient or slope of the dimensionless dependent variable with respect to the dimensionless independent variable according to the following equation [25]:

$$\text{Sensitivity} = \frac{\text{percentage change in output}}{\text{percetage change in input}} = \frac{\text{increment in output/ initial value of output}}{\text{increment in input/ initial value of input}} \quad \ldots\ldots. \quad (1)$$

This definition of sensitivity was used to investigate input and output parameters having different units. The sensitivity factor in this study represents change in the output parameter for 10% change in given input parameter. For example, a sensitivity factor of -5 means the percentage decrement of the output is 5% if the percentage increment of the given input is 10%, and is independent of the units of the input and output parameters.

2.1 Input parameters

Component geometry parameters

Figure 2 shows geometries of the five designs used in the present study. Starting with a thin-walled hollow structure, designs were evolved to evaluate sensitivity with changing part volume, thickness, height, layer surface area, and structural stiffness. Part wall thickness and Z-height are varied for the thin-walled designs (Design-I to IV) to estimate how process sensitivity will evolve with changing geometry. For the solid part design (V), percentage of porosity was varied instead of wall thickness to account for changes in volume. The values of the geometry parameters selected for sensitivity analysis are presented in Table 1.

Table 1: Component geometry parameters variations

Component geometry parameters	**Design I**	**Design II**	**Design III**	**Design IV**	**Design V**
Part wall thickness (mm)	2 1.5, 2, 2.5	1.5 1, 1.5, 2	1.5 1, 1.5, 2	1.5 1, 1.5, 2	-
Part geometry porosity (%)	-	-	-	-	30 0, 30, 60
Part Z-height (mm)	40 20, 40, 60	20 10, 20, 30	20 10, 20, 30	20 10, 20, 30	20 10, 20, 30

Process parameters

The printing process in MF^3 involves several input parameters. In the present study, a set of key parameters are studied. Table 2 presents typical values of selected process parameters based on experience. Layer thickness defines the height of each layer of printing. While a smaller layer thickness discretizes the build into higher resolution leading to better accuracy and surface quality, it leads to higher print time. Typically, a layer thickness of 0.2mm was used in MF^3. Variations to 0.1mm and 0.3mm was investigated for sensitivity in this study. Layer width define discretization of each layer in XY plane. Extrusion temperature defines the extruder temperature for softening the material just enough to overcome its viscosity and extrude through the nozzle smoothly. An extrusion temperature of 240ºC with variations to 220ºC and 260ºC was evaluated in this study. Build plate was heated to keep the substrate temperature high enough to enable efficient diffusion between two layers. It also provides slower cooling rate that helps minimizing part warpage. Influence of build plate temperature of 65ºC with variations to 45ºC and 85ºC is evaluated in this study. Printing speed defines the travel speed of nozzle while it extrudes material to print. As it directly defines print time, it is always desirable to get higher print speed. But it is limited by several parameters like material viscosity, filament stiffness to push through the nozzle, and print quality. Typically, a print speed of 10mm/s is used in MF^3 of Ti-6Al-4V. Variations to 5mm/s and 15mm/s was investigated for sensitivity in this study. Finally, two toolpath 0 – 90 and 45 – 135 were investigated in this study.

Table 2: Printing process parameters variations

Process parameters	**Variations**
Layer thickness (mm)	0.2 0.1, 0.2, 0.3
Layer width (mm)	0.48 0.36, 0.48, 0.60
Extrusion temperature (°C)	240 220, 240, 260
Build plate temperature (°C)	65 45, 65, 85
Printing speed (mm/s)	10 5, 10, 15
Toolpath (°)	0 – 90 0 – 90, 45 – 135

Powder-binder material properties

In this study, the properties used for Ti-6Al-4V in custom polymer binder were obtained from estimation models. The material definition for simulation includes mechanical and thermal properties over a range of temperature for the input material as shown in Table 3. The given material properties were varied to +/- 20% to investigate printing process sensitivity. These variations can be looked at as outcome of change in material formulation in terms of solids loading and custom polymer binder.

Table 3: Material properties variations

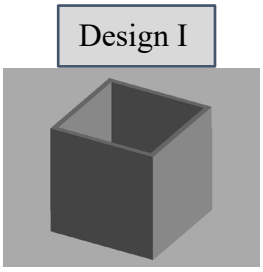
Material properties (at 23°C)	**Variations**
Thermal conductivity (mW/mm·°C)	1.466 1.1728, 1.466, 1.7592
Coefficient of thermal expansion (1/°C)	2.83E-05 2.26E-05, 2.83E-05, 3.40E-05
Specific heat capacity (mJ/t·°C)	8.95E+08 7.16E+08, 8.95E+08, 1.07E+09
Young's modulus (MPa)	205 164, 205, 246
Specific volume (mm^3/t)	3.38E+08 2.70E+08, 3.38E+08, 4.06E+08

2.2 Simulation setup: Base case for Design-I

In this study the finite element analysis (FEA) based simulations are conducted using Digitmat to estimate the outcome from MF^3 printing process. Table 4 lists the geometry, process parameters and material properties used in the simulation of base case for Design-I.

Table 4: Input for process simulation for the base case of Design-I

Input Variables		
Component geometry parameters	Part wall thickness	2mm
	Part Z-height	40mm
Process parameters	Layer thickness	0.1mm
	Layer width	0.48mm
	Extrusion temperature	$240^{o}C$
	Build plate temperature	$65^{o}C$
	Printing speed	5mm/s
	Toolpath	$0^{o} – 90^{o}$
Material properties	Thermal conductivity	1.466 mW/mm·C
	Coefficient of thermal expansion	2.83E-05 $1/^{o}C$
	Specific heat capacity	8.95E+08 $mJ/t\cdot^{o}C$
	Young's modulus	205 MPa
	Specific volume	3.38E+08 mm^3/t



2mm hollow cube 40mm x 40mm x 40mm

The CAD model of a 2mm thick hollow cube of size 40mm x 40mm x 40mm was imported in STL format. It was discretized into voxel mesh. The mesh size will have an influence on the prediction of the residual stresses, but a rather minor influence on the displacement results (warpage) [29]. However, the mesh size cannot be smaller than the layer thickness. Considering the computational time, a mesh size of 0.3mm was used. A GCode file from Simplify3D defines toolpath, layer thickness and printing speed. Other printing parameters like layer width, extrusion temperature, build plate temperature, chamber temperature, convection coefficient are defined through simulation tool graphical user interface as shown in Figure 3. The material definition includes the mechanical and thermal properties over a range of temperatures as shown in Figure 3.

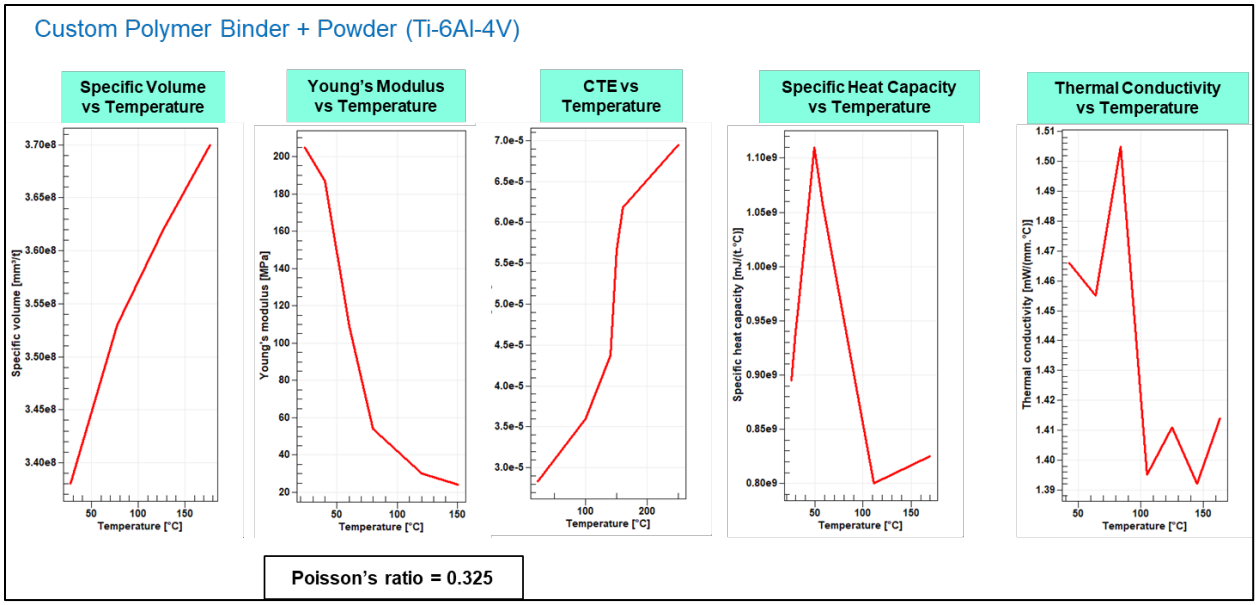


Figure 3. Mechanical and thermal properties of Ti-6Al-4V + polymer binder over a range of temperatures

Considering the computational time and number of simulation jobs, a layer-by-layer method activation method was used to simulate the printing process. Here, finite element layers are activated one at a time, whereas in filament discretization a chunk of filaments gets activated. Having defined the material, geometry and process inputs, the job was submitted for thermo-mechanical simulation.

3. RESULTS AND DISCUSSION

First, the results of Design-I base case are explained in detail. The simulation results are presented below for the individual output parameters, starting with print time, then deflection, Z-warpage, residual stress and substrate temperature. Then, the sensitivity analysis results of Design-I are discussed. Each of the input parameters was varied as discussed in previous section. For each individual variation, a simulation job was performed. The sensitivity factor (SF) was calculated using equation (1). Accordingly, the significance was termed 'high' for SF at levels >10, 'medium' in the range between 5 and 10, 'low' in the range between 1 and 5, and 'no' at levels <1.

Print time

Print time is an important aspect of any AM process. While lower print time indicates higher commercial viability, it is generally accompanied by quality compromise. Simulation provides an estimate of time required to print the given part under set process parameters. It is dependent upon component geometry parameters (part wall thickness, layer cross-sectional area, part maximum height) and process parameters (printing speed, part orientation/ build height, layer width, layer thickness). The estimated print time for the base case of Design-I was 60858s.

Deflection, all

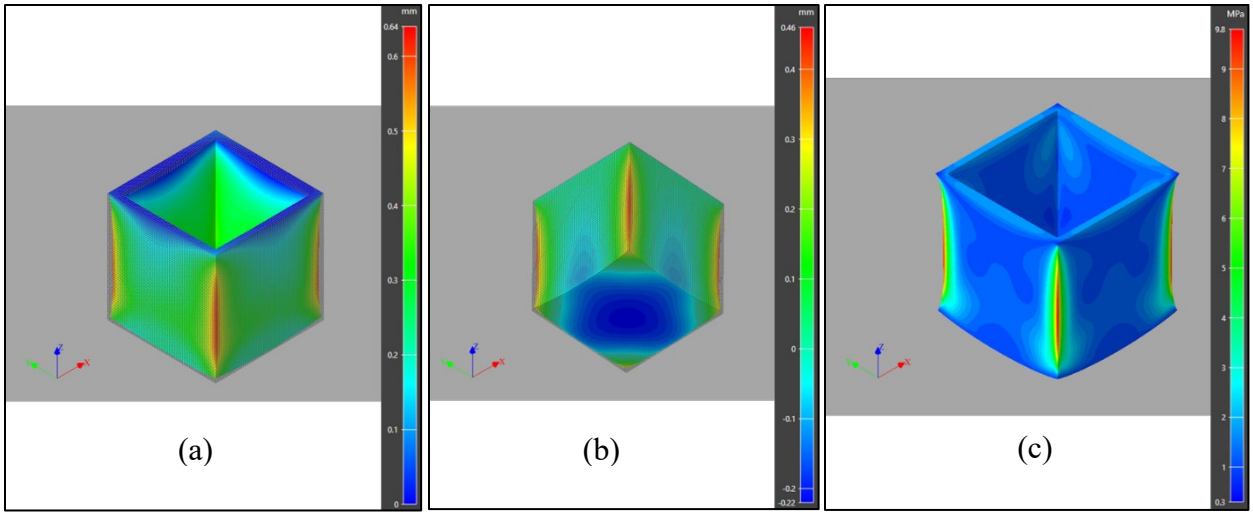


Figure 4. Design-I base case simulation results: (a) Deflection, all (b) Z-warpage (c) Residual stress (von Mises)

In MF^3 printing process, the material is subjected to softening/ partial melting while pushed through the extruder-nozzle, deposited on substrate layer-by-layer and then allowed to cool down and solidify. Afterwards, it is subjected to repeated cycles of heating and cooling with each new layer getting deposited. This leads to development of thermal gradient and inherent thermal strains in the printed part [29]. The extent of the strain varies according to coefficient of thermal expansion of the material. The thermal strain causes deflection and warpage, finally leading to deviations printed part dimensions opposed to defined CAD geometry. Hence, to achieve desired part quality and dimensional tolerances it is important to understand and control the deflection/ warpage phenomenon during MF^3 printing. Simulation provides an estimate of deflection in X, Y, Z direction as well as overall deflection (Deflection, all) results for given material, geometry and process parameters. It is primarily dependent upon temperature-related process parameters (extrusion temperature, build plate temperature) and material properties (coefficient of thermal expansion). The estimated maximum deflection (Deflection, all) for the base case of Design-I was 0.64mm as shown in Figure 4(a).

Z-warpage

As thermal strains lead to deflection in printed part, it is combined with nonuniform shrinkage resulting from nonuniform cooling due to layer-by-layer printing. This leads to warpage which is more significant across the printing plane along Z-axis. The estimated Z-warpage for the base case of Design-I was 0.69mm as shown in Figure 4(b).

Residual stress

The process simulation provides estimation of residual stress induced during and by end of the printing process due to non-uniform cooling. Figure 4(c) indicates von Mises stress as residual stress developed by the end that can be attributed to thermal gradient as a result of layer-by-layer stacking as well as differential heat loss from central zone compared to outer periphery. Lower thermal gradient, uniform and slower cooling helps in reducing residual stresses. The estimated von Mises stress for the base case of Design-I was 9.79MPa.

Substrate temperature

The simulation predicts the temperature history of the printing process by means of a transient thermal analysis. It is helpful to study the local temperature evolution during the process. Fig 5(a) shows the temperature variation indicating thermal gradient at the end of printing. The graph (b)

shows the history of temperature evolution oi the layer at 5mm height. It can be seen that the layer is extruded and deposited at set extrusion temperature of 240°C. However, by the time next layer is deposited, the previous layer cools down to 55°C.

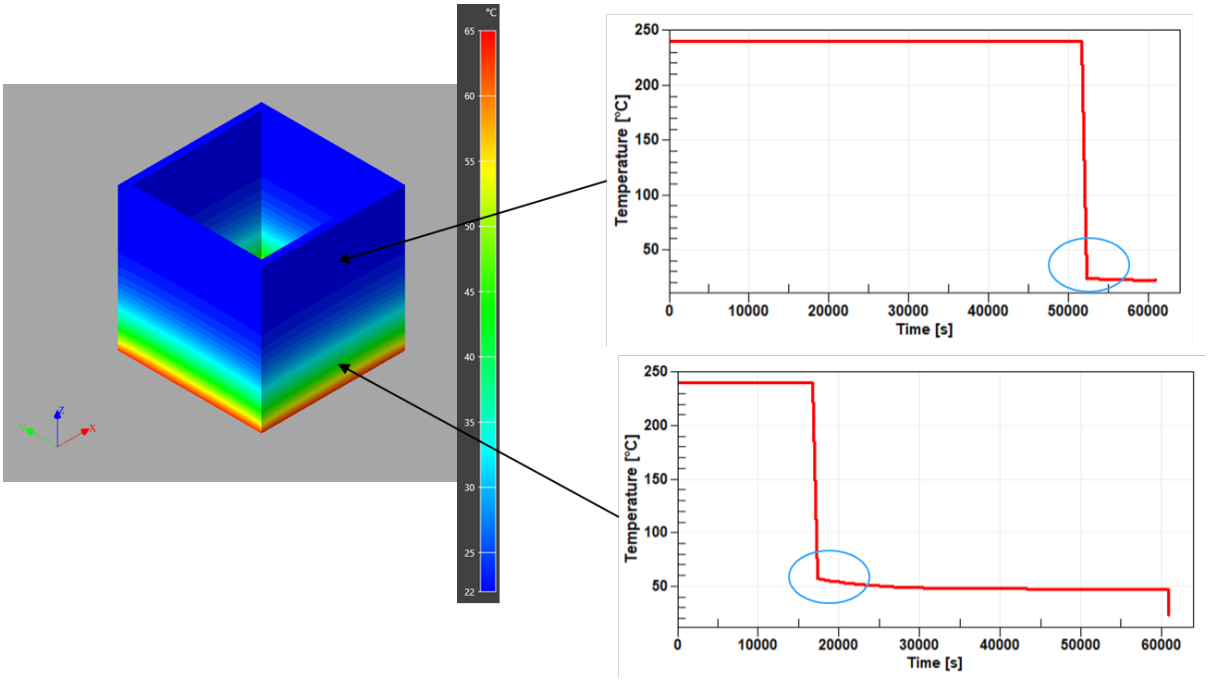


Figure 5. Design-I base case simulation results: (a) Temperature distribution (b) Substrate temperature at 35mm height (c) Substrate temperature at 5mm height

This is due to heat loss to the environment as an open chamber printer was considered in the study. The chamber temperature was set to ambient temperature, 20°C, in the simulation. However, the build plate was kept at 65°C. So, the printed layers were gaining heat from the heated bed. The heat flux depends upon the temperature gradient and thermal conductivity of the material. As a result of simultaneous heat loss and heat gain, the layer 5mm height is found to be at 55°C when the next layer comes in. We can say that the substrate temperature of this next layer is 55°C. Similarly, the graph (c) shows the history of temperature evolution in the layer at 35mm height. Here, the substrate temperature is found to be 22°C, which is close to the set chamber temperature 20°C. It this case the amount of heat gain from build plate was much lower than heat loss to environment. This is because of limited thermal conductivity of the material, while convection heat loss was more significant. The phenomenon of heat gain through conduction and heat loss through convection also depends upon surface area of exposure, Z-height, time taken to print each layer which ultimately depends on part geometry as well as printing parameters.

As build progresses, substrate temperature drops from 65°C (build plate temperature) to 20°C (ambient temperature). The importance of substrate temperature is that a lower substrate temperature leads to a lower amount of diffusion between two layers, hence, lower interlayer bond strength. Finally, a lower mechanical strength [27,28]. Hence, it is an important consideration not only from build setup or process parameters, but also from part and material design perspectives.

3.1 Sensitivity Analysis

As described, equation (1) provides the sensitivity factor (SF) calculation for every individual output parameter response to each variation of input parameters. Table 5 summarizes the SF results for Design-I. The sensitivity analysis provides means to identify significant input parameters for each of the output parameters. Sensitivity factor facilitates a quantitative yardstick to identify the significant parameters. A single SF is considered for each input-output combination for further analysis.

Table 5: Sensitivity factors (maximum) for Design-I

		Print Time	Max. Deflection	Max. Z-Warpage	Max. Residual Stress	Min. Substrate Temperature
Component geometry parameters	Part wall thickness	18.77	1.80	1.85	2.40	0.96
	Part Z-height	8.05	1.82	8.20	5.27	-6.67
Process parameters	Layer thickness	-19.65	-0.08	-0.19	-0.26	0.70
	Layer width	-18.56	-0.07	-0.11	-0.11	-0.13
	Extrusion temperature	0.00	17.06	17.25	16.78	0.32
	Build plate temperature	0.00	1.32	1.86	0.40	0.85
	Printing speed	-20.00	-0.07	-0.16	-0.16	0.70
	Toolpath	0.02	0.00	0.00	0.00	0.00
Material properties	Thermal conductivity	0.00	-0.12	-0.26	-0.16	1.08
	CTE	0.00	10.50	10.26	10.36	0.02
	Specific heat capacity	0.00	-0.05	-0.07	-0.08	0.45
	Young's modulus	0.00	0.00	0.00	10.00	0.00
	Specific volume	0.00	0.06	0.09	0.10	-0.52

Print time

According to the simulation results, print time was found to be sensitive to component geometry and process parameters. It was not influenced by any of the material properties. As part wall thickness increases, print time increases. A strong sensitivity was observed in print time towards part wall thickness. It was obvious that higher print area of each layer of the vertical walls and larger height of the bottom horizontal portion of the geometry led to larger print time. However, it was observed that print time increased even when wall thickness was reduced. This opposite response was difficult to understand logically. However, by investigating the toolpath it was learnt that in spite of same slicer setting when thickness was decreased to 1.5mm, a different infill with zig-zag path was generated which consumed more time, whereas in 2mm thickness, two straight line tracks formed the infill consuming lesser print time. Print time also showed high sensitivity to part Z-height or build height as number of layers vary proportionately. Print time is greatly influenced by layer thickness. Negative sign indicates that print increases when layer thickness decreases and vice versa. Part geometry having non-uniform cross-section along Z-axis, print time doesn't vary proportionately with layer thickness variation. Generally, layer width has significant influence on print time. With wider tracks, time to print infill of each layer decreases. However, in this design the thin walls are printed with minimal infill, hence no significant impact observed. Printing speed has a direct and significant influence on print time. Toolpath has negligible effect

on print time in this design. However, based on infill required, in some cases toolpath plays considerable role in print time. None of the variations in material properties had any influence on print time.

Deflection, all

The deflection results showed sensitivity to the three sets of input parameters to different extent. Low sensitivity was noted towards component geometry parameters like part wall thickness and Z-height. No variation was observed at increasing Z-height from 40mm to 60mm. In terms of printing process, layer thickness and layer width showed no influence on deflection. Extrusion temperature influences deflection strongly as it defines the thermal gradient. Higher extrusion temperature leads to higher deflection, and vice versa. Sensitivity to build plate temperature was low. Printing speed and toolpath showed no influence on deflection. From material properties, while coefficient of thermal expansion (CTE) showed strong effect, all other properties had no influence at all. This is because CTE defines volumetric changes with temperature change, which is used for deflection calculation in simulation.

Z-warpage

Z-warpage showed sensitivity pattern similar to deflection as the physical phenomenon and computational approaches are similar for both. While part wall thickness showed low sensitivity, part Z-height had considerable influence on Z-warpage. This is due to varying deflection in build direction with variation build height. On processing front, layer thickness and layer width showed no influence. Extrusion temperature influenced Z-warpage strongly, same as that for deflection. Higher extrusion temperature led to higher Z-warpage. Sensitivity to build plate temperature was low. Printing speed and toolpath showed no influence. From material properties, coefficient of thermal expansion (CTE) again showed strong effect, while all other properties had no influence at all.

Residual stresses

The residual stress results showed sensitivity to most of variables from the three sets of input parameters. On component geometry, while sensitivity was low to wall thickness, it was considerable to Z-height. Variation in Z-warpage leads to residual stress variations with varying height. Layer thickness and layer width had negligible impact. A strong sensitivity was observed towards extrusion temperature same as it was for deflection and warpage. Lower extrusion temperature will help reduce residual stresses. Build plate temperature, printing speed and toolpath showed negligible influence on residual stresses. For the first time, all the material properties showed some influence, though it was very small for thermal conductivity, specific heat and specific volume. Coefficient of thermal expansion (CTE) showed same amount of influence as it had on deflection and Z-warpage. Young's was found influential only towards residual stress results. As the residual stress is the result of resistance to deflection from material, it is proportionate with material stiffness. Hence, higher E and higher CTE value leads to higher residual stresses, and vice versa.

Substrate temperature

It was observed that substrate temperature showed sensitivity to most of input parameters from all three sets, though it was considerable only for a few input variables. From component geometry, wall thickness had negligible influence in this case. However, if part thickness will increase significantly, print time will increase. This allows more time to dissipate heat before next layer comes in, leading to lower substrate temperature. Highest sensitivity was observed towards part Z-height. As part height increases, substrate temperature decreases. As mentioned, greater amount of heat is lost to environment than heat gained from build plate. This is because of limited thermal

conductivity of the material, while convection heat loss was more significant, leading to lower temperature. While all the printing parameters showed some influence on substrate temperature, none of them was considerable enough in this case. Generally, build plate temperature has considerable influence up to certain build height. On material front, sensitivity was considerable for thermal conductivity, negligible for specific heat capacity and specific volume, and zero for CTE and Young's modulus.

4. CONCLUSIONS

The MF^3 of Ti-6Al-4V was analyzed for the first time using a systematic procedure based on sensitivity analysis principles. The procedure developed in this study was found to have the following key attributes:

1. The sensitivity analyses facilitated the identification of the dominant input parameters in MF^3 for the systems under consideration.
2. The quantitative relationships on the dependence of many MF^3 process output parameters on changes in component geometry, process parameters and material properties are presented.
3. The procedure clearly identified the relative importance of specific attributes of parts geometry, processing conditions, slicing strategies, powder-binder material properties based on the correlations between input parameters in each category and output parameters as process outcome.
4. The tool provides a powerful approach to identify the parameters that need to be optimized in the design stage and carefully monitored and controlled in the manufacturing stage of MF^3.
5. The insights gained on material-process-geometry interrelationships through the sensitivity study will enhance $DfMF^3$.
6. The present sensitivity analysis procedure is expected to be an invaluable tool not only for process optimization but also for going beyond from part design to materials development for MF^3.

5. ACKNOWLEDGEMENT

Authors acknowledge the financial support from Minority Business Development Agency, USA (MBDA) and National Aeronautics and Space Administration (NASA). The authors also recognize MSC Software (A Hexagon company) for providing the Digimat simulation tool used in this study.

6. REFERENCES

1. Joamin Gonzalez-Gutierrez, Santiago Cano, Stephan Schuschnigg, Christian Kukla, Janak Sapkota, Clemens Holzer, *Additive manufacturing of metallic and ceramic components by the material extrusion of highly-filled polymers: a review and future perspectives.* Materials 2018. 11(5): p. 840
2. Paramjot Singh, Qasim Shaikh, Vamsi K. Balla, Sundar V. Atre, Kunal H. Kate, *Estimating powder-polymer material properties used in design for metal fused filament fabrication ($DfMF^3$)*, JOM (2020) 72: 485.
3. Yvonne Thompson, Joamin Gonzalez-Gutierrez, Christian Kukla, Peter Felfer, *Fused filament fabrication, debinding and sintering as a low cost additive manufacturing method of 316L stainless steel,* Additive Manufacturing 30 (2019) 100861
4. Guohua Wu, Noshir A. Langrana, Rajendra Sadanji, Stephen Danforth, *Solid freeform fabrication of metal components using fused deposition of metals.* Materials & Design, 2002. 23(1): p. 97-105.

5. Walter Lengauer, Ivica Duretek, Markus Fürst, Viktoria Schwarz, et al., *Fabrication and properties of extrusion-based 3D-printed hardmetal and cermet components.* International Journal of Refractory Metals and Hard Materials, 2019. 82: p. 141-149.
6. Luquan Ren, Xueli Zhou, Zhengyi Song, Che Zhao, Qingping Liu, et al., *Process parameter optimization of extrusion-based 3D metal printing utilizing PW–LDPE–SA binder system.* Materials, 2017. 10(3): p. 305.
7. Seokyoung Ahn, Seong Jin Park, Shiwoo Lee, Sundar V. Atre, Randall M. German, *Effect of powders and binders on material properties and molding parameters in iron and stainless steel powder injection molding process*. Powder Technology 193 (2009) 162–169
8. Antonio Armillotta, Mattia Bellotti, Marco Cavallaro, *Warpage of FDM parts: experimental tests and analytic model*. Robotics and Computer–Integrated Manufacturing 50 (2018) 140–152
9. Pedram Parandoush, Dong Lin, *A review on additive manufacturing of polymer-fiber composites*. Composite Structures 182 (2017) 36–53
10. Rafael Quelho de Macedo, Rafael Thiago Luiz Ferreira, *Residual thermal stress in fused deposition modelling*, 24th edn. (2017), ABCM International Congress of Mechanical Engineering, Curitiba
11. Miquel Domingo-Espin, Josep M. Puigoriol-Forcada, Andres-Amador Garcia-Granada, Jordi Llumà, et al, *Mechanical property characterization and simulation of fused deposition modeling Polycarbonate parts.* Materials & Design 83 (2015) 670–677
12. Huanxiong Xia, Jiacai Lu, Sadegh Dabiri, Gretar Tryggvason, *Fully resolved numerical simulations of fused deposition modeling. Part I: fluid flow.* Rapid Prototyping Journal 24/2 (2018) 463–476
13. Yong Zhou Gang Xiong, Timo Nyberg, Dan Liu, *Temperature analysis in the fused deposition modeling process*. IEEE Computer Society ICISCE.2016.150
14. S.F. Costa, F.M. Duarte, J.A. Covas, *Thermal conditions affecting heat transfer in FDM/FFE: a contribution towards the numerical modelling of the process*. Virtual and Physical Prototyping, 2014. https://doi.org/10.1080/17452759.2014.984042.
15. Yizhuo Zhang, Y. Kevin Chou, *3D FEA simulations of fused deposition modeling process*. ASME International Conference on Manufacturing Science and Engineering, 2006. Ypsilanti, MI.
16. Alberto Cattenone, Simone Morganti, Gianluca Alaimo, Ferdinando Auricchio, *Finite element analysis of additive manufacturing based on fused deposition modeling (FDM): distortions prediction and comparison with experimental data*. Journal of Manufacturing Science and Engineering, 2018. https://doi.org/10.1115/1.4041626.
17. B. Barmore, *Fused Filament Fabrication of Filled Polymers for Metal Additive Manufacturing*. Mechanical Engineering, Oregon State University, 2016, pp. 55–60.
18. Tomas Webbe Kerekes, Hyoungjun Lim, Woong Yeol Joe, Gun Jin Yun, *Characterization of process–deformation/damage property relationship of fused deposition modeling (FDM) 3D-printed specimens*. Additive Manufacturing 25 (2019) 532–544
19. Filip Górski, Wiesław Kuczko, Radosław Wichniarek, *Influence of process parameters on dimensional accuracy of parts manufactured using fused deposition modelling technology*. Advances in Science and Technology Research Journal. DOI: 10.5604/20804075.1062340
20. J. Giannatsis, K. Sofos, V. Canellidis, D. Karalekas, V. Dedoussis, *Investigating the influence of build parameters on the mechanical properties of FDM parts*. Innovative Developments in Virtual and Physical Prototyping, Dec 2011. Publisher: CRC Press.
21. Gokulakrishnan Jothibabua, Saravana Kumar Gurunathanb, *Surrogate Based Sensitivity Analysis of Part Strength due to Process Parameters in Fused Deposition Modelling*. Procedia Computer Science 133 (2018) 772–778
22. B.H. Lee, J. Abdullah, Z.A. Khan, *Optimization of rapid prototyping parameters for production of flexible ABS object*, Journal of Materials Processing Technology 169 (2005) 54–61
23. Emily R. Fitzharris, Narumi Watanabe, David W. Rosen, Meisha L. Shofner, *Effects of material properties on warpage in fused deposition modeling parts*, The International Journal of Advanced Manufacturing Technology (2018) 95:2059–2070. https://doi.org/10.1007/s00170-017-1340-8

24. Bharath Vasudevarao, Dharma Prakash Natarajan, Mark Henderson, Anshuman Razdan, *Sensitivity of RP surface finish to process parameter variation*, https://www.researchgate.net/publication/2467464
25. Sundar.V. Atre, S.J. Park, R. Zauner, Randall M. German, *Process simulation of powder injection moulding: Identification of significant parameters during mould filling phase*, Powder Metallurgy (2007), 50:1, 76-85.
26. A. El Moumen, M. Tarfaoui, K. Lafdi, *Modelling of the temperature and residual stress fields during 3D printing of polymer composites*, The International Journal of Advanced Manufacturing Technology (2019) 104:1661–1676.
27. Q. Sun, G.M. Rizvi, C.T. Bellehumeur, P. Gu, *Effect of processing conditions on the bonding quality of FDM polymer filaments*, Rapid Prototyping Journal 14/2 (2008) 72–80.
28. Céline Bellehumeur, Longmei Li, Qian Sun, Peihua Gu, *Modeling of Bond Formation Between Polymer Filaments in the Fused Deposition Modeling Process,* SME Journal of Manufacturing Processes Vol. 6/No. 22004
29. e-Xstream, Digimat-AM simulation solution for Additive Manufacturing. https://www.e-xstream.com/product/digimat-am. Accessed 30 Dec 2019.
30. Alphastar, Genoa Additive Manufacturing design tool and software suite for polymers, metals and ceramics. http://www.alphastarcorp.com/products/genoa-3dp-simulation/. Accessed 30 Dec 2019.
31. Nikzad, M., S. Masood, and I. Sbarski, *Thermo-mechanical properties of a highly filled polymeric composites for fused deposition modeling.* Materials & Design, 2011. **32**(6): p. 3448-3456.